Talanta 87 (2011) 93–99

Contents lists available at SciVerse ScienceDirect

Talanta

journal homepage: www.elsevier.com/locate/talanta

Visual detection of organophosphorus pesticides represented by mathamidophos using Au nanoparticles as colorimetric probe

Hongkun Li[a,1], Jiajia Guo[a,1], Hong Ping[a], Lurui Liu[a], Minwei Zhang[a], Fengrui Guan[a], Chunyan Sun[a,*], Qian Zhang[b,**]

[a] Department of Food Quality and Safety, College of Quartermaster Technology, Jilin University, Changchun 130062, PR China
[b] College of Chemistry, Liaoning University, Shenyang 110036, PR China

ARTICLE INFO

Article history:
Received 30 May 2011
Received in revised form 9 September 2011
Accepted 15 September 2011
Available online 1 October 2011

Keywords:
Au nanoparticles
Colorimetric assay
Organophosphorus pesticides
Enzyme inhibition

ABSTRACT

With citrate-coated Au nanoparticles as colorimetric probe, a novel visual method for rapid assay of organophosphorus pesticides has been developed. The assay principle is based on catalytic hydrolysis of acetylthiocholine into thiocholine by acetylcholinesterase, which induces the aggregation of Au nanoparticles and the color change from claret-red to purple or even grey. The original plasmon absorption of Au nanoparticles at 522 nm decreases, and simultaneously, a new absorption band appears at 675 nm. The irreversible inhibition of organophosphorus pesticides on acetylcholinesterase prevents aggregation of Au nanoparticles. Under optimum conditions, the absorbance at 522 nm of Au nanoparticles is related linearly to the concentration of mathamidophos in the range of 0.02–1.42 μg/mL with a detection limit of 1.40 ng/mL. This colorimetric method has been successfully utilized to detect mathamidophos in vegetables with satisfactory results. The proposed colorimetric assay exhibits good reproducibility and accuracy, providing a simple and rapid method for the analysis of organophosphorus pesticides.

1. Introduction

Due to the high insecticidal activity, organophosphorus pesticides (OPs) with acute toxicity have been extensively used for pest control, which has raised serious public concern regarding the healthiness, environment and food safety [1]. By combining hydroxyl on active site serine of acetylcholinesterase (AChE), OPs can irreversibly inhibit the activity of AChE, thus leading to the loss of AChE hydrolysis for acetylcholine and *in vivo* accumulation of acetylcholine, thereby resulting in disturbance of cholinergic receptor activity which often causes respiratory paralysis and even death [2,3]. Therefore, rapid, efficient and reliable determination of trace levels of OPs has become increasingly important for public security and health protection, and related research is active.

Currently, the common methods for the analysis of OPs, such as gas chromatography (GC) [4–7] and high performance liquid chromatography (HPLC) [8,9] have been widely used for the determination of OPs with accurate results. These methods, however, require highly expensive instruments, complicated and time-consuming pretreatments, well trained operators, which limit their applications for on-site screening of these compounds [10,11]. With the emergence of nanotechnology, enzymatic biosensors for OPs detection have gained considerable attention due to the advantages of simplicity, rapidity, reliability, low cost devices, and on-field detection [12]. These nano-biosensors are based on the inhibition effects of OPs on acetylcholinesterase (AChE) activity, or the catalysis of organophosphorus hydrolase (OPH) on OPs hydrolysis. The catalytic activity of AChE for the hydrolysis reaction of acetylcholine to choline is drastically inhibited by trace amounts of OPs present in the environment. Nanomaterial-based AChE sensors have been extensively applied for AChE activity assay and OPs screening using different configurations and transduction technologies, such as electrochemistry (amperometry, potentiometry) [13], surface plasmon resonance (SPR) [14], absorption [15] and fluorescence spectroscopy [16,17]. With the implementation of nanomaterials including carbon nanotubes, Au nanoparticles (AuNPs), ZrO_2 nanoparticles, quantum dots (QDs) as immobilization matrices, dramatic enhancement in the electrocatalytic activity with very high sensitivity towards OPs detection has been achieved [13]. The localized surface plasmon resonance (LSPR) property of AuNPs covalently coupled with AChE has been applied for OPs determination [14]. The photoluminescent CdTe QDs has been integrated with AChE by the layer-by-layer (LbL) assembly

* Corresponding author. Tel.: +86 431 87836375; fax: +86 431 87835760.
** Corresponding author. Tel.: +86 24 62202378; fax: +86 24 62202378.
E-mail addresses: sunchuny@jlu.edu.cn, sunchy814@yahoo.com.cn (C. Sun), zhangqianlnu@gmail.com (Q. Zhang).
[1] These authors contributed equally to this work.

0039-9140/$ – see front matter © 2011 Elsevier B.V. All rights reserved.
doi:10.1016/j.talanta.2011.09.046

technique, resulting in a highly sensitive fluorescence biosensor for detection of OPs in vegetables and fruits based on enzyme inhibition mechanism [16]. The combination of catalytic effect of AChE and changes in surface state of nanoparticles could provide an optical signaling platform for OPs agents [15,17]. OPH can hydrolyze a large variety of OPs by producing less toxic products such as *p*-nitrophenol and diethyl phosphate, providing a direct biosensing route suitable for continuous OPs monitoring. Several types of OPH-based nano-biosensors have been introduced recently, including fluorescence [18–21] and amperometric ones [22]. Au nanoparticles (AuNPs) have received great attention in the development of visual sensing schemes owing to their intrinsic characteristics such as easy preparation, biocompatibility, stability, and high extinction coefficients [23,24]. The aggregation of AuNPs due to molecular recognition results in changes of their corresponding color and plasmon absorption. Depending on the unique distance-dependent optical properties, AuNPs have been widely applied as colorimetric probes for sensing of various substances, including viruses [25], proteins [26], DNA [27], cancerous cells [28], metal ions [29] and small molecules such as melamine [30–32].

In this work, using AuNPs as probe, we have established a rapid colorimetric assay method for OPs based on their inhibition on AChE (Scheme 1). The as-prepared AuNPs are claret-red and well-dispersed (1). Positively charged acetylthiocholine is employed as a substrate for AChE and is inclined to adsorb onto the surface of negatively charged AuNPs via electrostatic interactions (2). AChE catalyzes the hydrolysis of acetylthiocholine to produce thiocholine, which is positively charged and bears an additional thiol group (–SH). Due to this characteristic, thiocholine could prefer to substitute the citrate and easily bind onto the surfaces of AuNPs. As a result, crosslinking and aggregation of AuNPs would occur due to the electrostatic interactions and the strong Au–SH interaction (3), leading to the absorbance decrease of Au nanoparticles at 522 nm, and appearance of a new absorption band at 675 nm, accompanied by the color change of AuNPs from claret-red to purple or even grey. The presence of OPs can irreversibly inhibit the catalytic activity of AChE and the aggregation of AuNPs (4). Thus it is convenient to construct a sensitive, simple and economic method for rapid determination of OPs quantitatively with the plasmon absorption of AuNPs. Until now, to the best of our knowledge, there have been few reports on the detection of OPs in real food samples like fruits or vegetables using nano-biosensors [13,16,33]; hence, to apply the biosensors to OPs detection in real food samples remains a big challenge. Herein, our results demonstrate that the proposed optical biosensor using AuNPs as colorimetric probe can be applied to determine low concentrations of OPs in real vegetable sample with satisfactory results.

2. Experimental

2.1. Reagents and materials

$AuCl_3{\cdot}HCl{\cdot}4H_2O$, sodium citrate, vitamin C, vitamin B_1, vitamin B_2, $FeCl_3$, NaCl, $MgCl_2$, $ZnCl_2$, KCl, $CaCl_2$ and Na_3PO_4 were purchased from Beijing Chemical Reagent Company (Beijing, China). Acetylcholine chloride was obtained from Bio Basic Inc. (Toronto, Canada). Acetylthiocholine iodide (ATI), acetylcholinesterase (AChE, Type C3389, 500 U/mg from electric eel) and mathamidophos were purchased from Sigma–Aldrich (St. Louis, USA). Dithio-bis-nitrobenzoic acid (DTNB) and acetylcholine were purchased from Shanghai Sangon Biological Engineering Technology & Services Co., Ltd. All the chemicals were of analytical grade and triply distilled water was used in all experiments. Organic vegetables free from pesticides were purchased from the local supermarket.

2.2. Apparatus

Absorption spectra were recorded on a 2550 UV–vis Spectrophotometer (SHIMADZU Co., Japan). Transmission electron microscopy (TEM) measurements were made on a TECNAI F20 (FEI Co., Holland) operated at an accelerating voltage of 200 kV. The samples for TEM characterization were prepared by placing a drop of colloidal solution on carbon-coated copper grid and dried at room temperature. The photographs were taken with Caplio R6 digital camera.

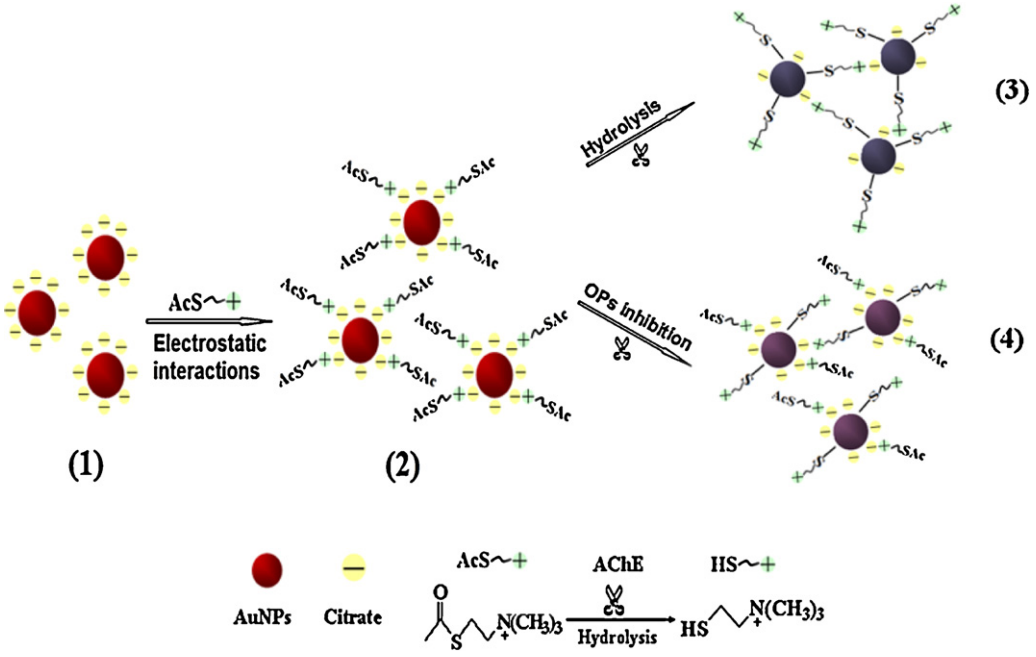

Scheme 1. Schematic illustration of rapid analysis of organophosphorus pesticides based on enzyme inhibition using Au nanoparticles as colorimetric probe.

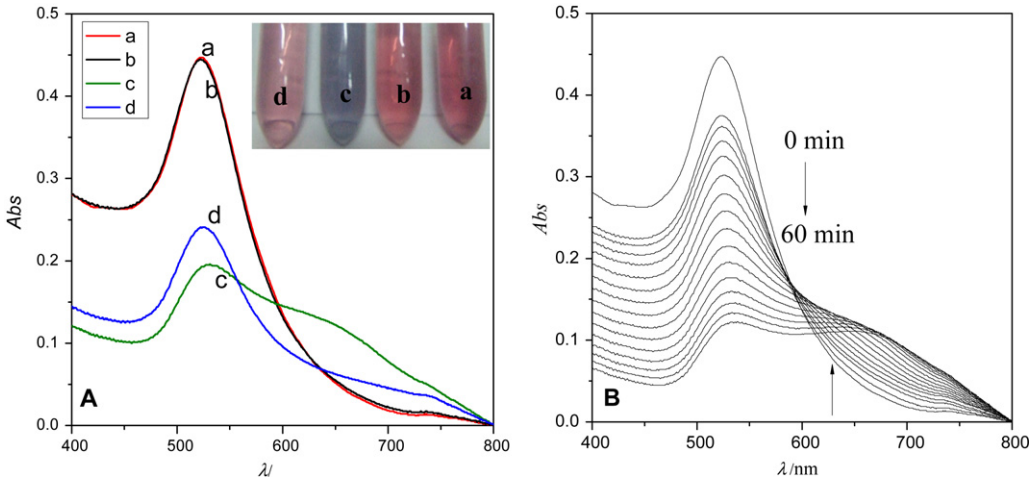

Fig. 1. (A) Absorption spectra and visual observation (Inset) of dispersed AuNPs (a), AuNPs after addition of ATI (15 μM, pH 8.0 PBS) (b), AuNPs after addition of ATI (15 μM, pH 8.0 PBS) and AChE (200 mU/mL) (c), AuNPs after addition of ATI (15 μM, pH 8.0 PBS), methamidophos (0.5 μg/mL) and AChE (200 mU/mL) (d). (B) Absorption spectra of AuNPs after addition of ATI (15 μM, pH 8.0 PBS) and AChE (200 mU/mL) recorded every 4 min.

2.3. Procedures

2.3.1. Preparation of AuNPs

The solution of 13 nm-diameter AuNPs was prepared according to the reference [34] and stored in a brown bottle at 4 °C. All glassware used in these preparations was thoroughly cleaned in aqua regia, rinsed in triply distilled water, and oven-dried prior to use. In a 250 mL round-bottom flask equipped with a condenser, 100 mL of 1 mM $HAuCl_4$ was heated to a rolling boil with vigorous stirring. Rapid addition of 10 mL of 38.8 mM sodium citrate to the vortex of the solution resulted in a color change from pale yellow to claret-red. Boiling was continued for 10 min; the heating mantle was then removed, and stirring was continued for an additional 15 min. After the solution cooled down to room temperature, it was filtered through a 0.4 μm Millipore membrane filter. The size and morphology of AuNPs were characterized by TEM.

2.3.2. Colorimetric detection of methamidophos

A typical colorimetric analysis of methamidophos was performed as follows. 0.9 mL AuNPs (diluted 5 times after preparation) and 0.1 mL ATI (pH 8.0 PBS) were added into 2 mL centrifuge tubes with 50 μL different concentrations of methamidophos or water, followed by addition of 10 μL AChE. The mixtures were incubated at 25 °C for 30 min. The UV–vis absorption spectra of the reacted solutions were recorded, and the calibration curve for methamidophos was established according to the absorbance of AuNPs at 522 nm (A_{522}).

2.3.3. Analysis of spiked vegetable samples

To measure methamidophos in the vegetable samples, Chinese cabbage was pretreated according to the reference [35]. 10 g of Chinese cabbage was weighed and finely chopped, then dissolved in 50 mL methanol and ultrasonicated for 60 min. The sample mixture was centrifuged and the supernatant was further filtered. The filtrate was further purified with activated carbon to remove impurities such as pigments. The obtained sample solution was washed with 10 mL methanol, and concentrated to almost dry at 50 °C by vacuum rotary evaporator. The residue was diluted with water to 5 mL. A certain amount of methamidophos was added into the Chinese cabbage, and pretreated in accordance with the above procedure; then, the extract was analyzed according to the method in Section 2.3.2.

The accuracy of the proposed rapid colorimetric biosensor for OPs detection in real contaminated vegetable sample was compared with enzyme inhibition rate method of Chinese National Standards GB/T 5009.199-2003 [36]. The standard detection method in GB/T5009.199-2003 is based on the principle that the hydrolyzate of acetylcholine catalyzed by AChE reacts with DTNB, forming a yellow substance with the maximum absorbance at 412 nm, whereas the presence of OPs can irreversibly inhibit the activity of AChE and decrease the absorbance at 412 nm.

3. Results and discussion

3.1. UV–vis absorption spectra and TEM images of AuNPs

The prepared AuNPs were monitored by the UV–vis absorption spectrum (Fig. 1A, curve a), which shows a unique sharp plasmon band at 522 nm, demonstrating that the obtained AuNPs are well-dispersed [37]. It can be seen from curve b in Fig. 1A that the addition of ATI (15 μM, pH 8.0 PBS) has no effects on the absorption spectrum of AuNPs and cannot induce color variation of the AuNPs solution. After AChE (200 mU/mL) is further added to the AuNPs–ATI system and incubated at 25 °C for 40 min, the original plasmon absorption of AuNPs at 522 nm decreases with the emergence of a new absorption band at 675 nm (Fig. 1A, curve c). Simultaneously, an obvious color change of the solution from claret-red to purple could be observed by naked eyes as displayed in the inset of Fig. 1A. Additionally, the absorption spectral variation of AuNPs becomes more and more obvious by prolonging the reaction time as shown in Fig. 1B. The spectral changes originate from AChE-catalyzed hydrolysis of ATI into thiocholine, leading to the aggregation of AuNPs as illustrated in Scheme 1. As the incubation time extended, more thiocholine could be generated by AChE-catalyzed hydrolysis of acetylthiocholine, in consequence, increased the aggregation degree and spectral variation of AuNPs. While AChE (200 mU/mL) was added to the AuNPs–ATI–methamidophos solution, the change of absorption spectrum could be hindered to some extent due to the inhibition of methamidophos on AChE activity (Fig. 1A, curve d). Moreover, the color differences among solutions of a, c and d are visual to naked eyes (Inset in Fig. 1A). Consequently, a rapid colorimetric method for OPs screening could be established using AuNPs as probe.

In order to know the morphology feature of the AuNPs before and after the occurrence of spectral and color change, the TEM images (Fig. 2) were obtained. The as-prepared AuNPs are well-dispersed with uniform particle size (Fig. 2A). The scale bar of the inset in Fig. 2A is 20 nm, which indicates that the particle diameter

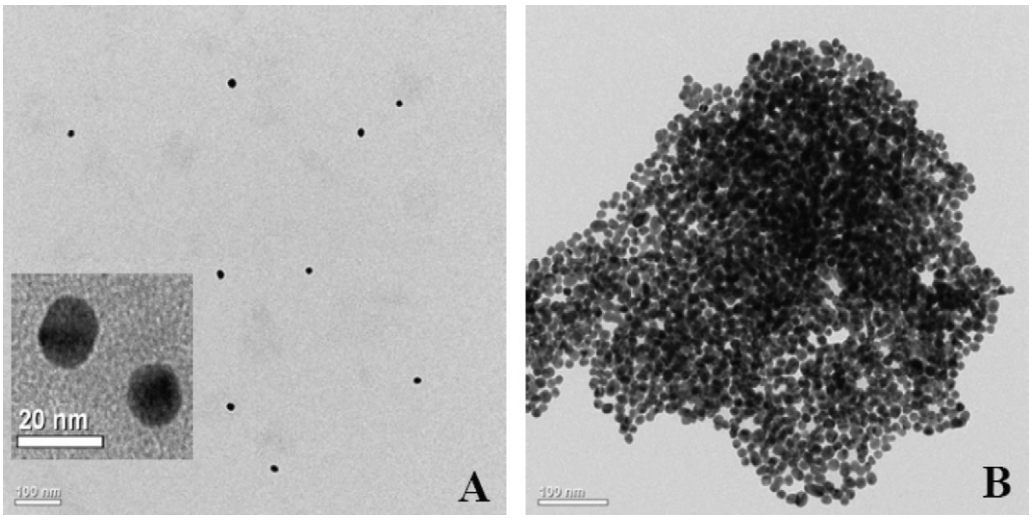

Fig. 2. TEM images of well-dispersed AuNPs (A) and AuNPs after addition of ATI (15 μM, pH 8.0 PBS) and AChE (500 mU/mL) (B). The inset in A is TEM image of AuNPs at the scale bar of 20 nm.

of AuNPs is about 13 nm. However, after addition of ATI and AChE, the AuNPs aggregate together (Fig. 2B). The results of TEM analysis are consistent with the UV–vis absorption spectra, and confirm directly the experimental observations discussed above. In order to further approach the analysis principle, a control experiment was performed under identical conditions using acetylcholine instead of acetylthiocholine as the substrate. There was no color change and absorption spectral variation even after the reaction mixture was incubated for 40 min. Acetylcholine and acetylthiocholine are similar in structure, which are catalyzed by AChE to produce choline and thiocholine respectively. According to the experimental results, consequently, it could be deduced that the thio of acetylthiocholine plays a critical role in aggregation of AuNPs, which provides further support for the analysis principle illustrated in Scheme 1.

3.2. Optimization of assay condition

As described above, the proposed rapid analysis for OPs is based on the spectral and color changes of AuNPs during the process of AChE-catalyzed hydrolysis of acetylthiocholine and OPs-induced inhibition on catalytic activity of AChE. Therefore, the performance of the developed OPs assay is strongly influenced by the assay conditions such as the pH of ATI, ATI concentration, AChE concentration and incubation time. Different assay conditions were optimized in our studies.

The pH of ATI solution could influence the performance of colorimetric assay. As shown in Fig. 3, ATI at pH 8.0 almost has no influence on the absorption spectrum of AuNPs, whereas ATI solutions with the other pH could induce the aggregation and spectral change of AuNPs. On the other hand, it is well known that the enzyme activity is highly pH dependent, since like all natural proteins, enzymes have a native tertiary structure that is sensitive to pH, and denaturation of enzymes can occur at extreme pH. Therefore, the pH of the solution containing the substrate, that is ATI, can affect the overall enzymatic activity. According to the characteristic of AChE provided by Sigma–Aldrich, the optimum pH of AChE activity is at pH 8.0. Consequently, the PBS of pH 8.0 was selected to prepare ATI solutions.

The effect of ATI concentration on the performance of colorimetric assay was investigated between 15 and 60 μM. It was found that excessive ATI could result in the aggregation and spectral change of AuNPs due to electrostatic interactions between positively charged acetylthiocholine and negatively charged AuNPs. Fig. 4 shows the plots of A_{522} versus the reaction time (0–80 min) for different concentrations of ATI. As shown in Fig. 4, during 0–80 min, ATI of 15 μM almost has no influence on AuNPs within the test time; however, given ATI concentration greater than 20 μM, A_{522} decreases with increased ATI concentration and prolonged time. In consequence, 15 μM ATI (pH 8.0 PBS) was used for colorimetric analysis in the following experiments.

The AChE activity and concentration have a great impact on the performance of colorimetric assay. The effect of AChE concentration on the response of the assay was examined in the range of 0–500 mU/mL, and the absorption spectra of the ensemble solution in each case were measured every 2 min. As anticipated, A_{522} decreases gradually with the reaction time, which is shown as Fig. 5. Additionally, the decline of A_{522} is more remarkable for the ensemble solution with a higher concentration of AChE. Given the higher concentration of AChE, the hydrolysis reaction could be completed within a shorter time. The insert photographs in Fig. 5 exhibit enhanced aggregation degree of AuNPs with the increase of AChE concentration. The experimental results indicate that the sensitivity as high as possible within a short time could be obtained when

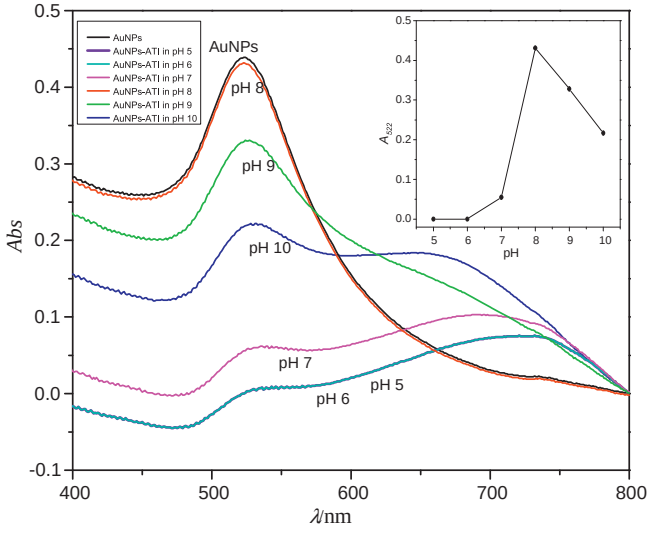

Fig. 3. Absorption spectra of AuNPs after addition of 15 μM ATI with different pH after incubation at 25 °C for 20 min. Inset: Variation of A_{522} of the AuNPs versus the pH of ATI.

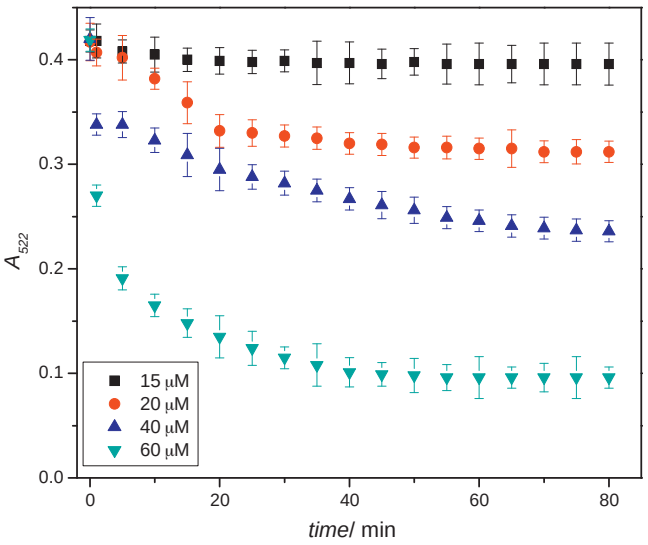

Fig. 4. Variation of A_{522} versus the reaction time for the AuNPs after addition of different concentrations of ATI (15, 20, 40, 60 μM in pH 8.0 PBS).

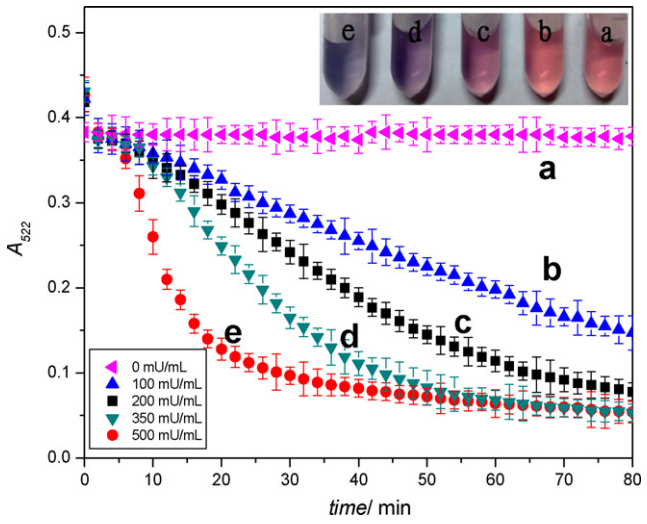

Fig. 5. Variation of A_{522} versus the reaction time for the AuNPs after addition of ATI (15 μM, pH 8.0 PBS) and different concentrations of AChE (0, 100, 200, 350, 500 mU/mL). The inset is the corresponding photographs of the ensemble solutions after incubation at 25 °C for 20 min.

using AChE of 500 mU/mL. For 500 mU/mL AChE, the aggregation and spectral variation of AuNPs could almost be completed within 30 min. Therefore, the incubation time throughout the following experiments was chosen as 30 min.

3.3. Interference studies

Interference studies were done in order to explore the specific detection of OPs in vegetables using the proposed colorimetric assay. These experiments included investigation of most commonly found substances in real samples of vegetables, such as vitamin C, vitamin B_1, vitamin B_2, Fe^{3+}, Na^+, Mg^{2+}, Zn^{2+}, K^+, Ca^{2+}, PO_4^{3-}. As shown in Fig. 6, no obvious interferences were noticed with the presence of these selected ions and compounds for determination of methamidophos (i.e. the relative error in all the cases was less than 6%). Therefore, the results showed no interferences from these substances in concentration levels usually found in vegetable samples.

3.4. Analytical performance and application of AuNPs-based sensing for methamidophos

The AChE-catalyzed hydrolysis of ATI into thiocholine could induce the aggregation of AuNPs with the color and spectral changes of the ensemble solution. In the presence of methamidophos, however, the color and spectral variation became slow after addition of AChE into AuNPs–ATI solution. The obstacles of methamidophos on the spectral changes originate from its inhibition on the catalytic activity of AChE. Under the optimal conditions, A_{522} is related linearly to the concentration of methamidophos in the range of 0.02–1.42 μg/mL with a detection limit of 1.40 ng/mL ($S/N = 3$). The relative standard deviation is 6.7% for the determination of 0.20 μg/mL methamidophos ($n = 7$), implying good reproducibility of the colorimetric assay. Compared with the traditional method, such as spectrophotometric and electrochemical method [38,39], the established colorimetric assay for OPs has the advantages of higher sensitivity, simpler sample pretreatment, faster analysis, and in particular, visual identification.

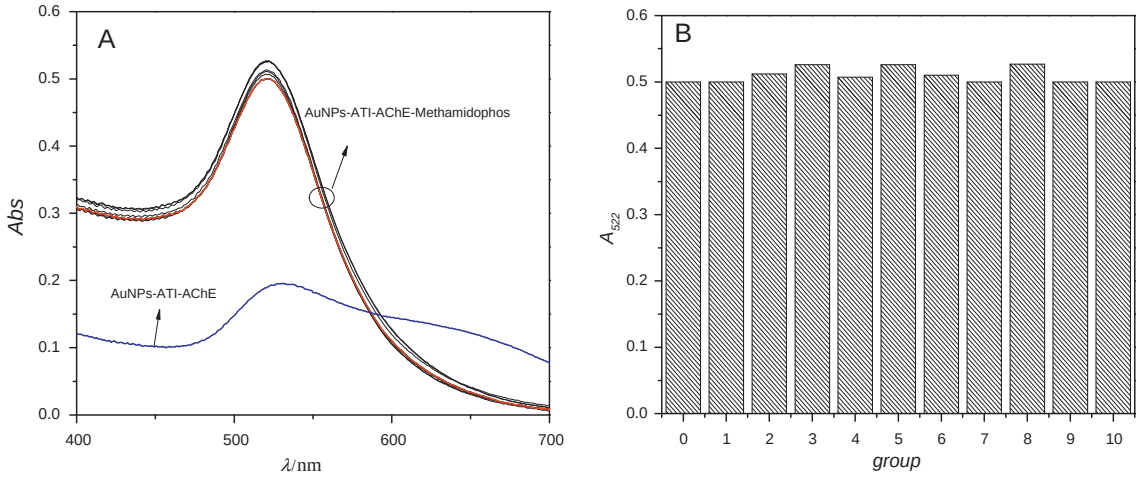

Fig. 6. Absorption spectra (A) and the corresponding A_{522} (B) of AuNPs–ATI–AChE in the presence of 2 μg/mL mathamidophos premixed with different substances. The red line is the absorption spectrum of AuNPs–ATI–AChE–mathamidophos and the blue line is the absorption spectrum of AuNPs–ATI–AChE. Substances: 0, control (AuNPs–ATI–AChE in presence of 2 μg/mL mathamidophos); 1, vitamin C (0.16 mg/mL); 2, vitamin B_1 (0.007 mg/mL); 3, vitamin B_2 (0.0013 mg/mL); 4, Fe^{3+} (0.019 mg/mL); 5, Na^+ (0.430 mg/mL); 6, Mg^{2+} (0.43 mg/mL); 7, Zn^{2+} (0.015 mg/mL); 8, K^+ (0.29 mg/mL); 9, Ca^{2+} (0.65 mg/mL); 10, PO_4^{3-} (0.55 mg/mL). (For interpretation of the references to color in this figure legend, the reader is referred to the web version of this article.)

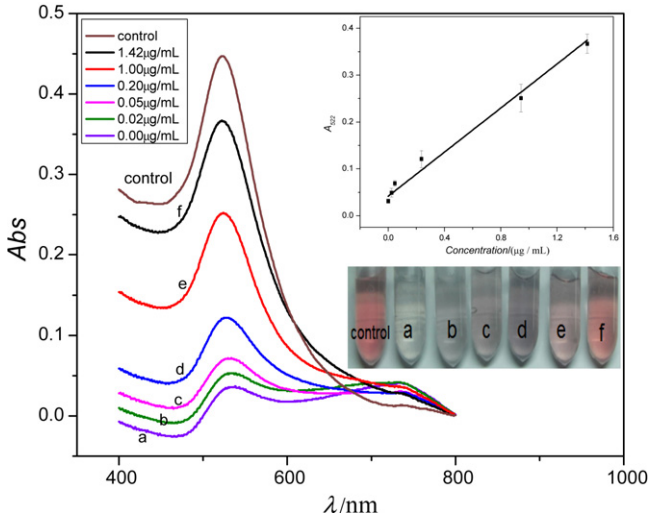

Fig. 7. Absorption spectra of the AuNPs spiked with known quantities of methamidophos to Chinese cabbage (0, 0.02, 0.05, 0.20, 1.00, and 1.42 μg/mL) after addition of ATI (15 μM, pH 8.0 PBS) and AChE (500 mU/mL). Inset: The calibration plot of methamidophos and photographs of the ensemble AuNPs solutions. AuNPs is taken as control.

To validate the proposed method to specifically detect methamidophos in vegetables, different amounts of methamidophos were added into Chinese cabbage, after that, the obtained spiked samples were pretreated and analyzed according to the procedure described in Sections 2.3.3 and 2.3.2. The calibration curve for methamidophos was obtained by detecting the sample extracts spiked with known quantities of methamidophos, as displayed in the inset of Fig. 7. According to this calibration curve, the recoveries in spiked Chinese cabbage vary from 90.2% to 111.3% and the results are listed in Table 1. Additionally, Fig. 7 shows the spectral and color variations of the ensemble AuNPs solutions in the absence and presence of different concentrations of methamidophos. Along with the increase of methamidophos concentration, the spectra and color

Table 1
Application of the proposed method for determination of methamidophos in Chinese cabbage spiked with different amounts of methamidophos.

Sample	Amount added (μg/mL)	Amount found (μg/mL)	(Recovery ± RSD) (%) (n = 3)
Chinese cabbage	0.047	0.052	111.3 ± 2.8
	0.235	0.213	90.2 ± 6.7
	0.943	0.869	92.2 ± 4.8

of the ensemble AuNPs solutions become closer to the original AuNPs (control). Methamidophos could inhibit AChE activity, thus the hydrolysis rate of acetylthiocholine would be decreased accompanied with less thiocholine formed. As a result, less aggregation of AuNPs could occur, combined with less absorption variation and less color change. Apparently, in the linear range of methamidophos from 0.02 μg/mL to 1.42 μg/mL, the color change of the ensemble AuNPs solutions can be distinguished by naked eyes (Inset in Fig. 7). The results indicate that the established visual method has promising feasibility for rapid screening of methamidophos in vegetables.

3.5. Comparison of the proposed colorimetric assay with enzyme inhibition rate of GB assay

With four types of vegetables as samples, we used the proposed colorimetric assay and the enzyme inhibition rate method of GB/T 5009.199-2003 to determine the content of methamidophos. The obtained results demonstrate that organic vegetables which are used as samples have no methamidophos contamination. In order to explore the application of the proposed colorimetric biosensor for OPs analysis in real sample, the vegetables free from OPs were immersed in 1 μg/mL methamidophos for 24 h, and then rinsed several times with distilled water. After that, the obtained samples were pretreated and analyzed according to the procedure described in Sections 2.3.3 and 2.3.2, at the same time, detected following the method of GB/T 5009.199-2003. The calibration curves for methamidophos of the two methods are illustrated in Fig. 8. As shown in Table 2, both of the proposed colorimetric assay and GB/T

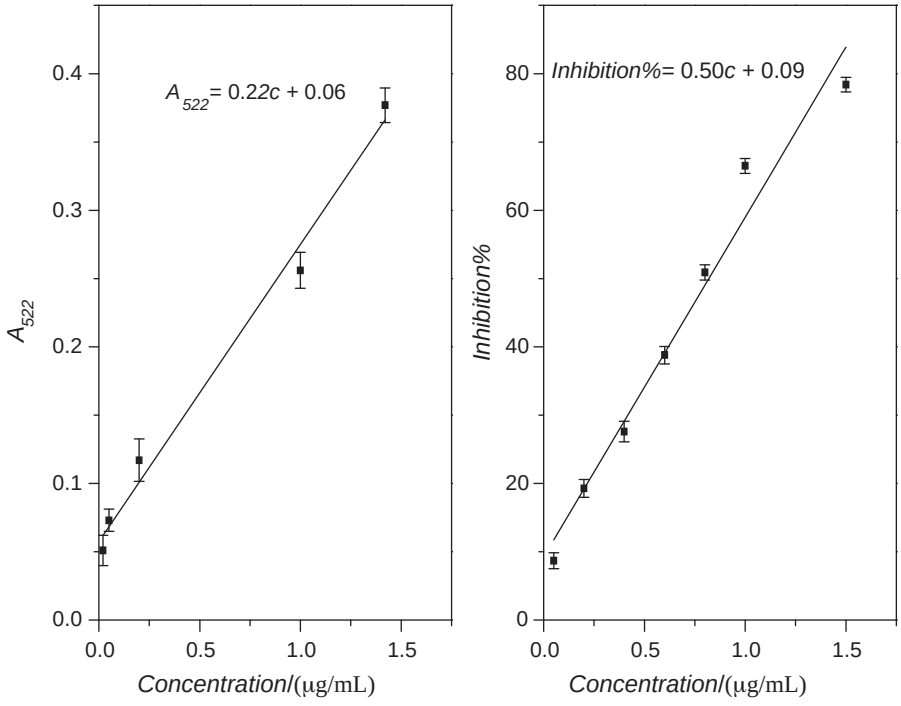

Fig. 8. The calibration plots for methamidophos of the proposed colorimetric assay and enzyme inhibition rate of GB assay.

Table 2
Comparison of analysis time, measured value, linear range, linear correlation coefficient and detection limit for methamidophos using different methods.

Method	The purposed method	GB/T 5009.199-2003
Analysis time (min)	30	30
Linear range (μg/mL)	0.02–1.42	0.05–1.50
Linear correlation coefficient (r)	0.9909	0.9868
Detection limit (μg/mL)	0.0014	0.018
Measured value of Chinese cabbage (μg/mL)	0.64	0.58
Measured value of cowpea (μg/mL)	0.60	0.59
Measured value of Chinese leek (μg/mL)	0.69	0.60
Measured value of cucumber (μg/mL)	0.71	0.61

5009.199-2003 method could be accomplished within 30 min for detection OPs. The obtained methamidophos content of the polluted vegetables from the two methods is in good accordance. The slight difference might be attributed to the different conditions and assay procedures. In addition, the proposed colorimetric assay has a lower detection limit and much higher sensitivity. Thus, the proposed method is credible for OPs detection and could be applied to rapid screening of OPs in real sample.

Similar to other biosensors including GB/T 5009.199-2003, which are based on the enzyme inhibition action of OPs on cholinesterases, the proposed colorimetric assay supplies the total amount of OPs in samples, and at this stage, is not capable to distinguish the different kinds of OPs. Due to the different inhibition effect of every OP on the same AChE, the sensor might show different response characteristic in presence of different type of OPs. Therefore, the simultaneous presence of various OPs in contaminated samples provides a challenge for the application for purely regulatory purposes where a specific analyte must be determined with a prescribed accuracy. Nevertheless, many advantages provided by the established sensor, such as easy sample pretreatment, rapid and visual analysis, high sensitivity, and low cost, could facilitate future development of rapid, high-throughput screening of OPs residues. This novel nano-biosensor might be used as an alarm system on-line and on site, which would provide either quantification of one contaminant when this analyte is present alone or an indication of total contamination of particular samples.

4. Conclusions

In summary, a sensitive, rapid and simple visual assay to detect OPs has been developed using citrate-coated AuNPs as colorimetric probe. AChE-catalyzed hydrolysis of acetylthiocholine into thiocholine, leading to the aggregation of AuNPs with spectral and color changes, which could be hindered by OPs due to their inhibition on AChE activity. Taking methamidophos as the representative pesticide, the visual detection of OPs in vegetables using AuNPs as colorimetric probe has been achieved with satisfactory results. The whole analysis could be accomplished within 30 min, which can meet the needs for on-site rapid monitoring of trace OPs in vegetables. The proposed assay for OPs can be observed by the naked eyes and measured by UV–vis spectrophotometer, therefore no sophisticated instruments are required for the assay. The possible disadvantage of this biosensor is that it cannot distinguish different kinds of OPs and thus lacks enough selectivity. Nevertheless, many advantages provided by the established sensor, such as easy sample pretreatment, rapid and visual analysis, high sensitivity, and low cost, could facilitate future development of rapid, high-throughput screening of OPs residues.

Acknowledgments

This work was financially supported by the National Natural Science Foundation of China (No. 20905031; No. 20901035) and the research startup fund of Jilin University (No. 4305050102H6).

References

[1] L.H. Wang, L. Zhang, H.L. Chen, Prog. Chem. 18 (2006) 440–452.
[2] Y.H. Lin, F. Lu, J. Wang, Electroanalysis 16 (2004) 145–149.
[3] X. Sun, X.Y. Wang, Biosens. Bioelectron. 25 (2010) 2611–2614.
[4] Q. Xiao, B. Hu, C.H. Yu, L.B. Xia, Z.C. Jiang, Talanta 69 (2006) 848–855.
[5] Y.S. Su, J.F. Jen, J. Chromatogr. A 1217 (2010) 5043–5049.
[6] M.K. Chai, G.H. Tan, Food Chem. 117 (2009) 561–567.
[7] L.J. Qu, H. Zhang, J.H. Zhu, G.S. Yang, H.Y. Aboul-Enein, Food Chem. 122 (2010) 327–332.
[8] T. Pérez-Ruiz, C. Martinez-Lozano, V. Tomas, J. Martin, Anal. Chim. Acta 540 (2005) 383–391.
[9] C.P. Sanz, R. Halko, Z.S. Ferrera, J.J.S. Rodriguez, Anal. Chim. Acta 524 (2004) 265–270.
[10] S. Andreescu, L. Barthelmebs, J.L. Marty, Anal. Chim. Acta 464 (2002) 171–180.
[11] M. Del Carlo, A. Pepe, M. Sergi, M. Mascini, A. Tarentini, D. Compagnone, Talanta 81 (2010) 76–81.
[12] S.Q. Liu, L. Yuan, X.L. Yue, Z.Z. Zheng, Z.Y. Tang, Adv. Powder Technol. 19 (2008) 419–441.
[13] A.P. Periasamy, Y. Umasankar, S.M. Chen, Sensors 9 (2009) 4034–4055.
[14] T.J. Lin, K.T. Huang, C.Y. Liu, Biosens. Bioelectron. 22 (2006) 513–518.
[15] M. Wang, X.G. Gu, G.X. Zhang, D.Q. Zhang, D.B. Zhu, Langmuir 25 (2009) 2504–2507.
[16] Z.Z. Zheng, Y.L. Zhou, X.Y. Li, S.Q. Liua, Z.Y. Tang, Biosens. Bioelectron. 26 (2011) 3081–3085.
[17] T. Yu, J.S. Shen, H.H. Bai, L. Guo, J.J. Tang, Y.B. Jiang, J.W. Xie, Analyst 134 (2009) 2153–2157.
[18] C.A. Constantine, K.M. Gattas-Asfura, S.V. Mello, G. Crespo, V. Rastogi, T.C. Cheng, J.J. DeFrank, R.M. Leblanc, J. Phys. Chem. B 107 (2003) 13762–13764.
[19] X.J. Ji, J.Y. Zheng, J.M. Xu, V.K. Rastogi, T.C. Cheng, J.J. DeFrank, R.M. Leblanc, J. Phys. Chem. B 109 (2005) 3793–3799.
[20] A.L. Simonian, T.A. Good, S.S. Wang, J.R. Wild, Anal. Chim. Acta 534 (2005) 69–77.
[21] C.A. Constantine, K.M. Gattás-Asfura, S.V. Mello, G. Crespo, V. Rastogi, T.C. Cheng, J.J. DeFrank, R.M. Leblanc, Langmuir 19 (2003) 9863–9867.
[22] D. Du, W.J. Chen, W.Y. Zhang, D.L. Liu, H.B. Li, Y.H. Lin, Biosens. Bioelectron. 25 (2010) 1370–1375.
[23] Z.X. Wang, L.N. Ma, Coord. Chem. Rev. 253 (2009) 1607–1618.
[24] W.A. Zhao, M.A. Brook, Y.F. Li, Chembiochem 9 (2008) 2363–2371.
[25] K. Niikura, K. Nagakawa, N. Ohtake, T. Suzuki, Y. Matsuo, H. Sawa, K. Ijiro, Bioconjug. Chem. 20 (2009) 1848–1852.
[26] A. Laromaine, L.L. Koh, M. Murugesan, R.V. Ulijn, M.M. Stevens, J. Am. Chem. Soc. 129 (2007) 4156–4157.
[27] M. Cho, M.S. Han, C. Ban, Chem. Commun. 38 (2008) 4573–4575.
[28] C.D. Medley, J.E. Smith, Z. Tang, Y. Wu, S. Bamrungsap, W.H. Tan, Anal. Chem. 80 (2008) 1067–1072.
[29] L. Li, B.X. Li, Y.Y. Qi, Y. Jin, Anal. Bioanal. Chem. 393 (2009) 2051–2057.
[30] L. Li, B.X. Li, D. Cheng, L.H. Mao, Food Chem. 122 (2010) 895–900.
[31] B. Roy, A. Saha, A.K. Nandi, Analyst 136 (2011) 67–70.
[32] X.S. Liang, H.P. Wei, Z.Q. Cui, J.Y. Deng, Z.P. Zhang, X.Y. You, X.E. Zhang, Analyst 136 (2011) 179–183.
[33] A. Amine, H. Mohammadi, I. Bourais, G. Palleschi, Biosens. Bioelectron. 21 (2006) 1405–1423.
[34] K.C. Grabar, R.G. Freeman, M.B. Hommer, M.J. Natan, Anal. Chem. 67 (1995) 735–743.
[35] T. Pérez-Ruiz, C. Martínez-Lozano, V. Tomás, J. Martín, Talanta 54 (2001) 989–995.
[36] Chinese National Standards GB/T5009.199-2003, Rapid Determination for Organophosphate and Carbamate Pesticide Residues in Vegetables, Standards Press of China, Beijing, 2003.
[37] L.P. Sun, J.F. Zhang, H. Li, X.Y. Wang, Z.W. Zhang, S. Wang, Q.Q. Zhang, Chem. J. Chinese U. 30 (2009) 95–99.
[38] N. Deng, Y.N. Ni, K. Sergec, Chin. J. Chem. 28 (2010) 404–410.
[39] Y.R. Li, Z.Y. Gan, Y.F. Li, Q. Liu, J.C. Bao, Z.H. Dai, M. Han, Sci. China Chem. 53 (2010) 820–825.